A Comparative Study between Shielded and Open Coplanar Waveguide Discontinuities

N. I. Dib[1], W. P. Harokopus, Jr.[2], G. E. Ponchak[3], and L. P. B. Katehi[1]

[1]Department of EECS, University of Michigan, Ann Arbor, Michigan 48109

[2]Texas Instruments, Dallas, Texas 75070

[3]NASA Lewis Research Center, Cleveland, Ohio 44135

ABSTRACT

A comparative study between open and shielded coplanar waveguide (CPW) discontinuities is presented. In this study, the space domain integral equation method is used to characterize several discontinuities such as the open-end CPW and CPW series stubs. Two different geometries of CPW series stubs (straight and bent stubs) are compared with respect to resonant frequency and radiation loss. In addition, the encountered radiation loss due to different CPW shunt stubs is evaluated experimentally. The notion of *forced radiation* simulation is presented, and the results of such a simulation are compared to the *actual* radiation loss obtained rigorously. It is shown that such a simulation cannot give reliable results concerning radiation loss from printed circuits. © 1992 John Wiley & Sons, Inc.

INTRODUCTION

Coplanar waveguide (CPW) is rapidly becoming the transmission line of choice in high-frequency applications and is successfully competing against the microstrip which has been the primary structure for hybrid and monolithic circuits. Due to many years of microstrip use, a large body of published data and CAD software pertaining to low- and high-frequency microstrip circuit and antenna design has been widely available. In contrast, models for shielded or open coplanar waveguide circuit design are still under development [1–21]. In addition, there is little data available concerning the radiation loss from CPW discontinuities [7,12,19]; therefore, there are no guidelines for low-loss, high-frequency CPW design. Nevertheless, despite this scarcity of reliable circuit models, CPW has provided an attractive alternative to conventional microstrip lines at high frequencies due

to many appealing properties [22–27]. These include the ability to wafer probe, and the ease in connecting shunt lumped elements or devices without using via holes. Such advantages arise because both conducting surfaces (the center conductor and the ground plane) are on the same side of the dielectric substrate.

Another important characteristic of coplanar waveguides is that the line impedance and phase velocity are less dependent on the substrate height than on the aspect ratio (slot width/center conductor width). Since the conducting surfaces of a CPW structure are all printed on the same interface, careful design could efficiently confine the fields to this interface. This characteristic benefits both shielded and open CPW lines as it provides control over leakage and unwanted parasitic coupling. Printed lines which are not enclosed in a metallic package, such as the feed network of a monolithic array, tend to radiate power in the

form of space and surface waves. In conventional monolithic lines, the level of parasitic radiation is strongly affected by the electric thickness of the substrate, which complicates high-frequency design due to little flexibility in choosing appropriate substrate structures. Since mechanical considerations put a lower limit on the physical thickness of integrated circuit substrates, it is difficult to avoid excessive loss when operating above 100 GHz in lines such as the microstrip where the field penetrates the whole substrate. In contrast, in coplanar waveguides the substrate thickness plays a lesser role; the fields are concentrated in the slots and are better confined on narrow apertures. Since the dimensions of the slots are limited only by photolithographic techniques, coplanar waveguides have more flexibility in design and, therefore, greater potential for low radiation loss and low dispersion.

However, even if coplanar waveguides radiate much less than a microstrip operating at the same frequency, as this frequency enters the submillimeter-wave region, the radiation loss increases and complicates the design. As a result, further reduction of parasitic radiation is required. A way to achieve this and be able to extend the operation of a coplanar waveguide into the submillimeter-wave region is to generate a surface-wave–free environment. This is possible with the use of a matched dielectric lens which has been exploited effectively to excite aperture-type radiating elements [28,29]. In such a structure, as in almost all CPW circuits, air-bridges (or bond wires) are used to connect the ground planes in order to suppress the coupled slotline mode. These air-bridges can be characterized by either using a rigorous full wave analysis [10,16,17,20] or a hybrid technique [11,14].

In this article, shielded and open CPW discontinuities will be analyzed using the space domain integral equation (SDIE) technique [8,9,12,30]. This method has shown excellent versatility in the study of a wide range of planar elements, and its accuracy has been demonstrated by comparison to measurements performed on a variety of open and shielded structures. The integral equation is formulated in terms of equivalent magnetic currents flowing on the slot apertures, as opposed to the full-wave technique presented in refs. [1,6,19], where an integral equation in terms of the electric current on the conducting surfaces is formed. The former technique is more appropriate for CPW problems where the ground planes approach the boundary surfaces, while the latter better fits
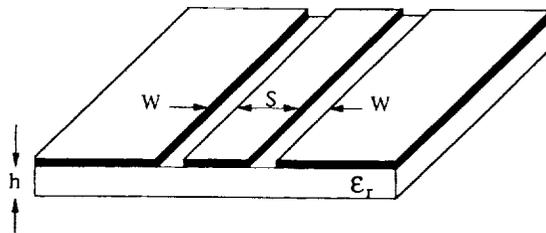

Figure 1. A generic geometry of a conventional coplanar waveguide structure.

problems having finite size conductors. The SDIE technique, as presented here, accurately takes into account all loss mechanisms by employing the appropriate Green's functions. Specifically, in the case of open coplanar waveguide discontinuities, the open space Green's function is expressed in terms of Sommerfield integrals so that radiation in the form of space and surface waves is accurately evaluated. This is in contrast to techniques used elsewhere [31,32], which simulate open space by setting the cover resistance to 377 Ω (forced radiation). Resonant properties and radiation losses for a number of shielded and open CPW stub discontinuities will be presented and guidelines for design will be given.

2. THEORY

A generic geometry for a conventional coplanar waveguide structure is shown in Figure 1. The dielectric layers supporting the coplanar structure are considered lossless and the conducting surfaces have zero ohmic loss. The two-slot apertures have width W and are separated by a distance S. With the application of the equivalence principle, the two slots can be replaced by equivalent magnetic currents $(\vec{M}_s^+, \vec{M}_s^-)$ flowing on a perfectly conducting surface which covers the slot apertures (see Fig. 2). These magnetic currents radiate electric fields, which are continuous across the surface
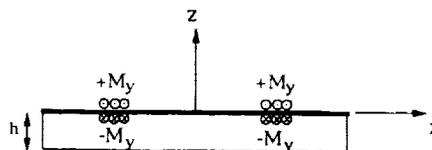
Figure 2. The equivalent problem obtained after the application of the Equivalence Principle. Only the longitudinal component of the surface magnetic current density is shown here.

36

of the slot apertures, as shown by the following equations:

$$\vec{M}_s^+ = -\vec{M}_s^- = \vec{M}_s \qquad (1)$$

with

$$\vec{M}_s^+ = \vec{E}_s \times \hat{a}_z \qquad z \geq 0 \qquad (2)$$

$$\vec{M}_s^- = \vec{E}_s \times (-\hat{a}_z) \qquad z \leq 0 \qquad (3)$$

where $\vec{E}_s$ is the electric field in the slot apertures. Furthermore, continuity of the magnetic fields on the slot apertures results in the expression

$$\hat{a}_z \times [\vec{H}^+(\vec{M}^+) - \vec{H}^-(\vec{M}^-)] = \hat{a}_z \times \vec{H}^{inc} \qquad (4)$$

where $\vec{H}^+(\vec{M}^+)$ and $\vec{H}^-(\vec{M}^-)$ are the magnetic fields radiated above and below the slots, respectively, and $\vec{H}^{inc}$ is the incident magnetic field exciting the CPW line. The magnetic fields may be expressed in terms of the unknown equivalent magnetic currents through a first-order Fredholm integral equation:

$$\vec{H}^{\pm} = \int\int_{S_{CPW}} [k_{\pm}^2 \vec{I} + \vec{\nabla}\vec{\nabla}] \\ \cdot \vec{\Gamma}_m^{\pm}(\vec{r}/\vec{r}') \cdot \vec{M}_s^{\pm}(\vec{r}')\, ds'. \qquad (5)$$

In eq. (5), S_{CPW} is the surface of the slot apertures and $k_{\pm}^2$ and $\vec{\Gamma}_m^{\pm}$ are the wavenumbers and magnetic field dyadic Green's functions in the regions above and below the CPW slots, respectively. The space domain integral eq. (4) is solved numerically using the Method of Moments [33]. In this solution scheme, the equivalent magnetic currents flowing on the slot apertures are expanded into a summation of piecewise sinusoidal basis functions, as shown:

$$\vec{M}(x', y')$$
$$= \sum_{i=x,y} \hat{a}_i \sum_{n_i=1}^{N_i+1} \sum_{m_i=1}^{M_i+1} [V_{n_i m_i}]^T [\phi_{n_i m_i}(x', y')] \qquad (6)$$

where $[V_{n_i m_i}]^T$ is the transposition of the vector of unknown current coefficients, and $[\phi_{n_i m_i}(x', y')]$ is the vector of the known basis functions. These functions are considered to be separable with respect to x' and y' parameters and have the following form:

$$\phi_{n_x m_x}(x', y') = f_{n_x}(x')g_{m_x}(y') \qquad (7)$$

$$\phi_{n_y m_y}(x', y') = f_{n_y}(y')g_{m_y}(x') \qquad (8)$$

with

$$f_{n_x}(x')$$
$$= \begin{cases} \dfrac{\sin[\xi(x' - x_{n_x-1})]}{\sin(\xi \ell_x)} & x_{n_x-1} \leq x' \leq x_{n_x} \\ \dfrac{\sin[\xi(x_{n_x+1} - x')]}{\sin(\xi \ell_x)} & x_{n_x} \leq x' \leq x_{n_x+1} \\ 0 & \text{elsewhere} \end{cases} \qquad (9)$$

$$g_{m_x}(y') = \begin{cases} 1 & y_{m_x} \leq y' \leq y_{m_x+1} \\ 0 & \text{elsewhere} \end{cases} \qquad (10)$$

where ℓ_x is the subsection length and ξ the wave number in the dielectric. The functions $f_{n_y}(y')$ and $g_{m_y}(x')$ are given by eqs. (9) and (10) with x, x', y, and y' replaced by y, y', x, and x', respectively.

In view of eqs. (6) and (7), and with the application of Galerkin's method, equation (4) takes the matrix form:

$$[Y_{mn}^{\nu\mu}][V_{nm}^{\nu\mu}] = [I_{\nu\mu}] \qquad (11)$$

with $Y_{mn}^{\nu\mu}$ the elements of the admittance matrix, $I_{\nu\mu}$ the elements of the excitation vector, and V_{nm} the amplitude coefficients for the magnetic current expansion functions. The excitation of the CPW structures is provided by ideal current sources appropriately placed on the slot apertures [8,9]. The solution of the matrix eq. (11) results in the evaluation of the equivalent magnetic currents and, consequently, the electric fields in the slots. From the field distribution, the network parameters may be computed by transmission line theory assuming that a single mode (the coplanar mode) is excited along the feeding lines [8,9]. For example, the input impedance of a one port CPW discontinuity can be evaluated from the positions of the minima and maxima of the electric field standing wave in the feeding lines. These minima and maxima positions may be obtained accurately by applying cubic spline fit on the field distribution derived through the method of moments. Such a technique has been successfully used previously, and has shown very good accuracy in characterizing multiport planar discontinuities [8,9,30,34].

The integral equation method, as it has been outlined above, applies to open and shielded problems in exactly the same way. What makes the solution of these two problems different is the form of the Green's function and the computational considerations required for its numerical

37

evaluation. Issues associated with the accurate evaluation of the Green's function and the complexities introduced by its form in the open and shielded CPW structures will be discussed in detail in following sections. The Green's function included in the integral eq. (5) is the electric vector potential produced by a unit magnetic current source and, as such, satisfies all the appropriate conditions on the boundary surfaces surrounding the volume of interest. Specifically, in *open* CPW problems, the magnetic field satisfies the radiation condition:

$$\lim_{\vec{r} \to \infty} \vec{r} \left(\frac{\partial \vec{H}}{\partial \vec{r}} - jk\vec{H} \right) = 0 \qquad (12)$$

while, in the case of *shielded* CPW, the spatial spectral components of the magnetic field given by eq. (5) satisfy the following equation on the cavity walls:

$$\hat{n}_w \times (\vec{\nabla} \times \vec{H}_k) = \mathbf{Z}^k_{sw} \cdot \vec{H}_k \qquad (13)$$

where k indicates the order of the spatial spectral field components, $\hat{n}_w$ is the vector normal to the walls toward the interior of the cavity, and $\mathbf{Z}^k_{sw}$ is the surface impedance dyad [35] for the kth spatial spectral component. In the case of perfectly conducting walls this dyad becomes identical to zero, while for resistive walls it becomes complex. The surface impedance spectral dyad is uniquely specified by the boundary conditions of the problem under study, and for this reason is restricted in form. This implies a very limited choice of values which could simulate physically realizable boundaries. Furthermore, there are no values for these spectral dyads, which could accurately simulate free space. Attempts to force radiation in shielded problems by arbitrarily choosing the spectral dyads can lead to quite inaccurate and inconclusive results, specifically with respect to radiation loss for circuit elements and radiation resistance for antenna elements. In the following sections, we discuss issues associated with the Green's function in shielded and open CPW and will also address the approach of *forced radiation*.

2.1. Shielded Coplanar Waveguides

When the CPW structure under study is shielded by a cavity (see Fig. 3), the excited electromag-
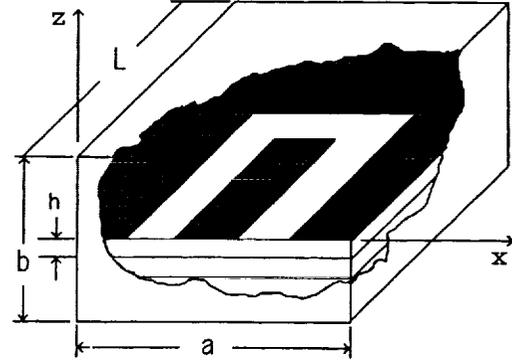
Figure 3. A coplanar waveguide shielded by a cavity filled with several dielectric layers.

netic field can be decomposed into a discrete infinite set of spectral solutions, each one satisfying the appropriate boundary conditions on the cavity walls. Similarly, the modified Green's function pertinent to the corresponding boundary value problem is a dyad

$$\overline{G}^{\pm}_m = G^{\pm}_{xx} \hat{x}\hat{x} + G^{\pm}_{yx} \hat{y}\hat{x} + G^{\pm}_{yy} \hat{y}\hat{y} + G^{\pm}_{xy} \hat{x}\hat{y} \qquad (14)$$

which is defined as

$$\overline{G}^{\pm}_m = [k^2_{\pm}\overline{I} + \vec{\nabla}\vec{\nabla}] \cdot \overline{F}^{\pm}_m (\vec{r}/\vec{r}'). \qquad (15)$$

Each component of $G^{\pm}_m$ is a superposition of infinitely many discrete solutions and, consequently, can be written into the form of a double infinite sum of PG (Pincherle–Goursat) type, as shown below [8,9]

$$G^+_{xx}(\vec{r}/\vec{r}')$$

$$= \sum_{m=0}^{\infty} \sum_{n=0}^{\infty} \frac{2e_n}{aL} \frac{1}{k^2_{z+} - k^2_+} [k^2_x P_+ + k^2_y Q_+]$$

$$\sin(k_x x')\cos(k_y y')\sin(k_x x)\cos(k_y y) \quad (16)$$

$$G^+_{yx}(\vec{r}/\vec{r}') = \sum_{m=1}^{\infty} \sum_{n=1}^{\infty} \frac{4}{aL} \frac{k_x k_y}{k^2_{z+} - k^2_+} \cdot [P_+ - Q_+]$$

$$\sin(k_x x')\cos(k_y y')\cos(k_x x)\sin(k_y y) \quad (17)$$

$$G^+_{xy}(\vec{r}/\vec{r}') = \sum_{m=1}^{\infty} \sum_{n=1}^{\infty} \frac{4}{aL} \frac{k_x k_y}{k^2_{z+} - k^2_+} [P_+ - Q_+]$$

$$\cos(k_x x')\sin(k_y y')\sin(k_x x)\cos(k_y y) \quad (18)$$

38

$$G_{yy}^+(\bar{r}/\bar{r}')$$

$$= \sum_{m=0}^{\infty} \sum_{n=0}^{\infty} \frac{2e_m}{aL} \frac{1}{k_{z+}^2 - k_+^2} [k_y^2 P_+ + k_x^2 Q_1]$$

$$\cos(k_x x')\sin(k_y y')\cos(k_x x)\sin(k_y y) \quad (19)$$

where

$$P_+ = \left(\frac{k_{z+}}{\omega\mu_+}\right) \frac{\omega\mu_+ + jk_{z+} \, Z_+^{LSE} \tan(k_{z+} \, d_+)}{k_{z+} \, Z_+^{LSE} + j\omega\mu_+ \tan(k_{z+} \, d_+)}$$

$$(20)$$

$$Q_+ = \left(\frac{\omega\epsilon_+}{k_{z+}}\right) \frac{k_{z+} + j\omega\epsilon_+ \, Z_+^{LSM} \tan(k_{z+} \, d_+)}{\omega\epsilon_+ \, Z_+^{LSM} + jk_{z+} \tan(k_{z+} \, d_+)}$$

$$(21)$$

$$\begin{aligned} e_n &= 1 & n &= 0 \\ &= 2 & n &\neq 0 \end{aligned} \quad (22)$$

$$\begin{aligned} e_m &= 1 & m &= 0 \\ &= 2 & m &\neq 0 \end{aligned} \quad (23)$$

$$k_x = \frac{m\pi}{a} \quad (24)$$

$$k_y = \frac{n\pi}{L} \quad (25)$$

$$k_+^2 = \omega^2\mu_+\epsilon_+ \quad (26)$$

$$k_+^2 = k_{z+}^2 + k_x^2 + k_y^2 \quad (27)$$

where d_+, μ_+, and ϵ_+ are the thickness, permeability, and permittivity of the dielectric layer directly above the slot aperture. In the above expressions, G_{ij}^+ denotes H_i^+ at $z = 0$ due to an infinitesimal M_j at $z' = 0$, where $i, j = x, y$. In addition, Z_+^{LSE} and Z_+^{LSM} are the LSE and LSM input impedances seen at $z = d_+$, which can be computed using transmission line theory. That is, each layer (except the ones surrounding the slot aperture) is replaced by an ideal transmission line with a characteristic impedance (Z_0^{LSE} or Z_0^{LSM}) and an eigenvalue, k_{z_i}, where

$$k_{z_i}^2 + k_y^2 + k_x^2 = \omega^2\mu_i\epsilon_i$$

$$(Z_0^{LSE})^i = \frac{\omega\mu_i}{k_{z_i}}$$

$$(Z_0^{LSM})^i = \frac{k_{z_i}}{\omega\epsilon_i}$$

The components of G_m^- are given by equations similar to eqs. (16)–(27) [8,9].

In the expressions for the modified Green's function, as given by (16)–(27), the summations over m and n are theoretically infinite. For the numerical solution of the integral equation, these summations are truncated, and the number of terms kept depends on the convergence behavior of the admittance matrix. Due to the nature of the problem solved here, the above summations have a convergence behavior similar to summations described elsewhere [34]. In the present work, the number of terms in the summations and the number of basis functions are chosen so that convergence of the scattering parameters of the coplanar waveguide discontinuity is achieved [8,9].

2.2. Open Coplanar Waveguides

When the cavity of a shielded CPW is moved to infinite, the environment surrounding the structure becomes open permitting real power to leak to free-space in the form of radiation modes (*space waves*) or guided modes (*surface and leaky waves*). From these two types of generated electromagnetic waves, the former have a continuous spectrum, while the latter a discrete one. As a result, the infinite summations in the shielded CPW case, which are characteristic of the Green's functions and the corresponding excited fields, turn into infinite integrals of Sommerfeld type. In the simplest case of an open CPW printed on a dielectric substrate of thickness h and with a dielectric constant, ϵ_r (see Fig. 1), the components of the magnetic-field dyadic Green's function, $\bar{F}_m^-$, are in the form [36]:

$$F_{xx}^- = F_{yy}^- = \frac{1}{j\omega \, 2\pi\mu_0} \int_0^\infty J_0(\lambda\rho) \frac{\lambda}{u}$$

$$\frac{u \cosh[u(h + z)] + \epsilon_r\mu_0 \sinh[u(h + z)]}{f_1(\lambda, \epsilon_r, h)} d\lambda$$

$$(28)$$

$$F_{zx}^- = \cot(\phi) \, F_{zy}^- = -\frac{1 - \epsilon_0\epsilon_r}{j\omega \, 2\pi\mu_0} \cos(\phi)$$

$$\int_0^\infty J_1(\lambda\rho) \frac{\sinh(uz)}{\lambda^2 \, f_1(\lambda, \epsilon_r, h) \, f_2(\lambda, \epsilon_r, h)} d\lambda. \quad (29)$$

The functions, $f_1(\lambda, \epsilon_r, h)$ and $f_2(\lambda, \epsilon_r, h)$, are the characteristic equations for the surface waves, TE

and TM, to the dielectric interface, and are given by:

$$f_1(\lambda, \epsilon_r, h) = \epsilon_r u_0 \cosh(uh) + u \sinh(uh) \quad (30)$$

$$f_2(\lambda, \epsilon_r, h) = u_0 \sinh(uh) + u \cosh(uh) \quad (31)$$

$$u_0^2 = \lambda^2 - \omega^2 \mu_0 \epsilon_0 \quad (32)$$

$$u^2 = \lambda^2 - \omega^2 \mu_0 \epsilon_0 \epsilon_r. \quad (33)$$

This formulation allows for a dielectric substrate or half space of any dielectric constant, thus, the components of $\overline{F}_m^+$ can also be obtained from the same equations.

For the solution of eq. (11), most of the computation effort is spent on the evaluation of the elements of the admittance matrix. The complexity in these computations comes from the Sommerfeld integration as it is combined with multiple space integrals. As a result, these integrals are computed using a special treatment, which consists of numerical and analytical techniques as described elsewhere [36,37].

2.3. Forced Radiation

There has been an attempt to model radiation loss from printed circuits by setting the resistance of the top wall of the shielding box to 377 Ω [31,32]. As noted above, such an attempt can lead to quite inaccurate and inconclusive results. In fact, forced radiation simulations may predict a loss factor much larger than the "actual" one, which can only be obtained through a rigorous analysis of the open structure [32]. This is due to the fact that there are no values for the surface impedance dyad in eq. (13) which could accurately simulate free-space environment. In the next section, a CPW series stub inside a box with the resistance of the lower and bottom walls set to 377 Ω will be analyzed. Radiation loss predicted from such a simulation will be compared to the "actual" radiation loss. In addition, it will be shown that the distance at which these walls are positioned is a critical parameter that affects the derived results considerably.

3. NUMERICAL EXAMPLES

Figure 4 shows the normalized capacitive reactance for an open-end CPW discontinuity of shielded and open type. The results for the two
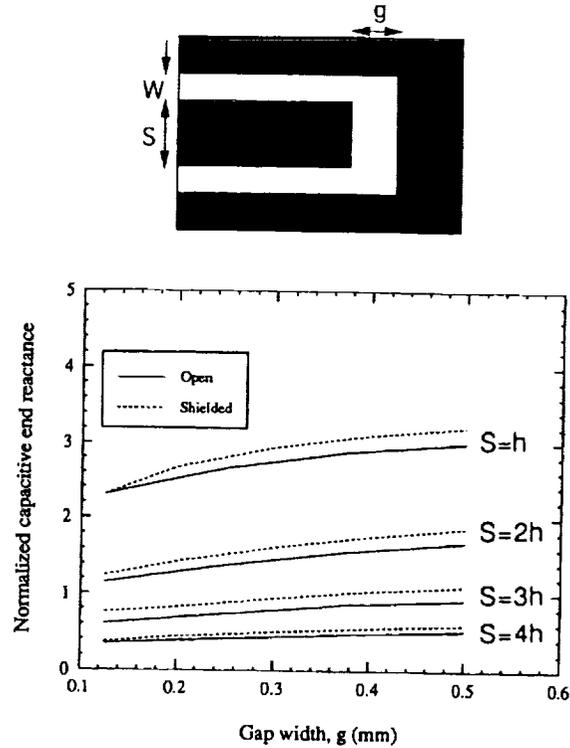
Figure 4. Normalized capacitive end reactance of an open-end CPW; $W = 0.25$ mm, $h = 0.5$ mm, and $\epsilon_r = 13.1$

cases are in good agreement, differing only by the amount of power radiated into the substrate and free space. The radiation loss from this one-port discontinuity (Fig. 5) increases with the gap width and the center conductor width.

Two series stub geometries are shown in Figure 6, and the magnitude of S_{12} of both stubs with a mean length of 1.35 mm is given in Figure 7. This
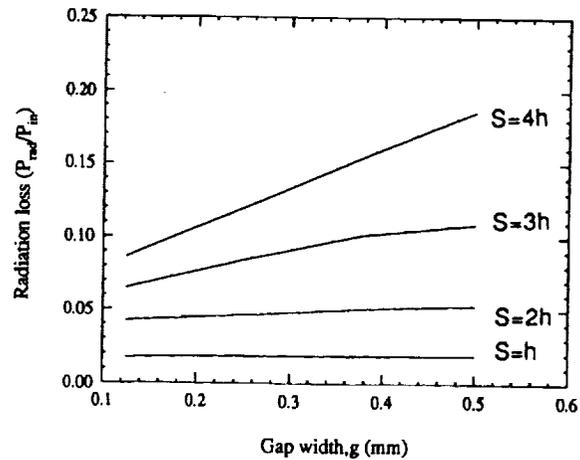
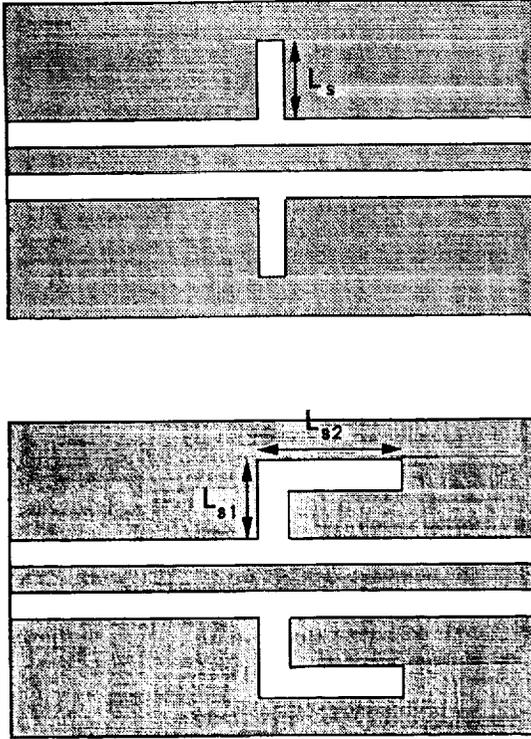**Figure 5.** Radiation loss of a CPW open-end discontinuity. Dimensions are the same as in Figure 4.

40

Figure 6. Two different CPW series stub geometries.

plot indicates that the stub geometry may affect the resonant frequency by as much as 7%. Specifically, the straight stub has a resonance at about 22 GHz, while for the bent geometry the resonance is 1.5 GHz higher. The sharper resonance of the nonshielded bent stub indicates lower radiation loss than the straight stub. As shown in
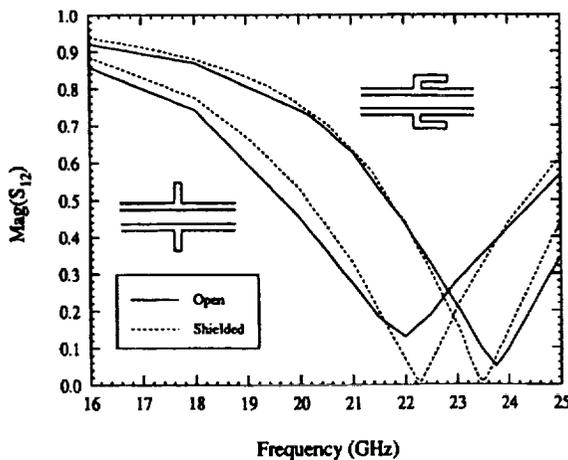

Figure 7. Mag(S_{12}) of the CPW series stub geometries with mean length of 1.35 mm, $W = 0.225$ mm, $S = 0.45$ mm, $h = 0.635$ mm, $\epsilon_r = 9.9$, $L_s = 1.35$ mm, $L_{s1} = 0.45$ mm, and $L_{s2} = 1.125$mm.
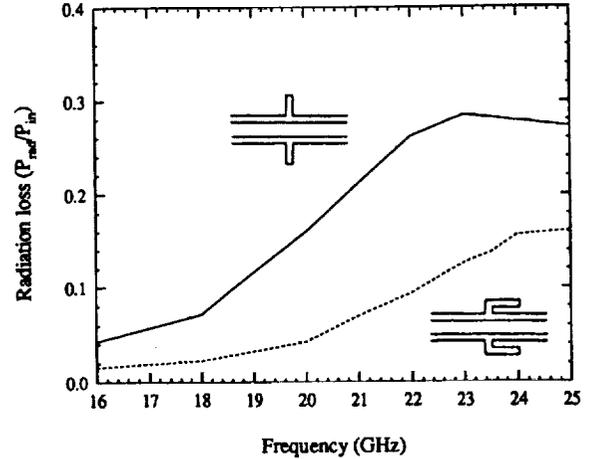

Figure 8. Radiation loss, $1 - |S_{11}|^2 - |S_{12}|^2$, of the CPW series stub geometries. Dimensions are the same as in Figure 7.
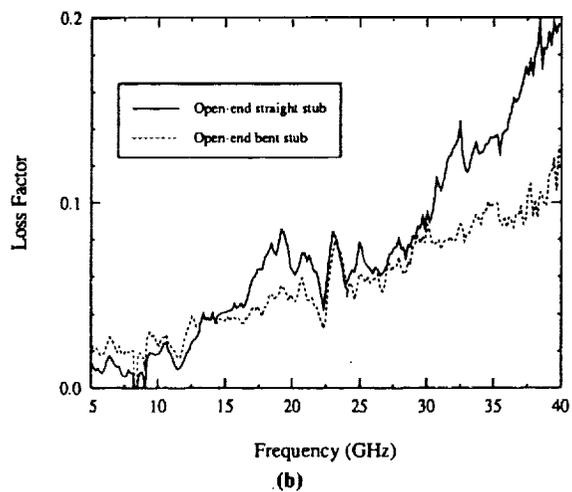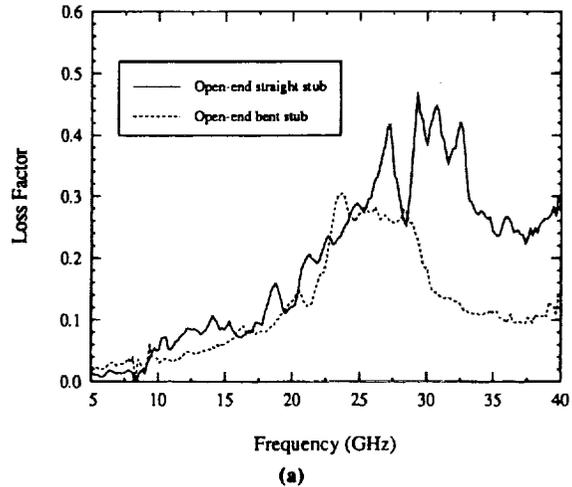
diation loss than the straight stub. As shown in Figure 8, the straight stub experiences severe loss which exceeds 25% of the input power. The parasitic radiation is high in this example because the electric fields in the two-stub slots are in phase, and thus they radiate constructively. In contrast, the electric fields in the bent geometry are 180° out of phase.

Four different CPW shunt stubs are shown in Figure 9, where air-bridges are used to connect the ground planes of the CPW stub in order to prevent the excitation of the coupled slotline mode. A comprehensive theoretical and experimental study of these stubs has been performed [11,38]; however, for illustration purposes, only the measured radiation loss of the open-end stubs will be presented here. Figure 10 shows the measured loss factor of these stubs, which includes radiation, conductor, and dielectric losses. Since the stubs are all of the same length, a comparison of the loss factor can provide a measure of the radiation loss. It can be noticed that loss is maximum at the resonant frequency for all stubs, which agrees with the radiation behavior of microstrip stubs above resonance [30]. Furthermore, the loss factor for straight stubs is larger than that for bent stubs. This is due to the fact that, in the case of bent stubs, the fields radiated by the coupled slotline modes in the two opposing stubs partially cancel. It can be seen also that the air-bridges reduce radiation loss by shorting out the coupled slotline model in the CPW stubs. But, it is still noted that the straight stubs have increasing radiation loss after the first resonant frequency.

41
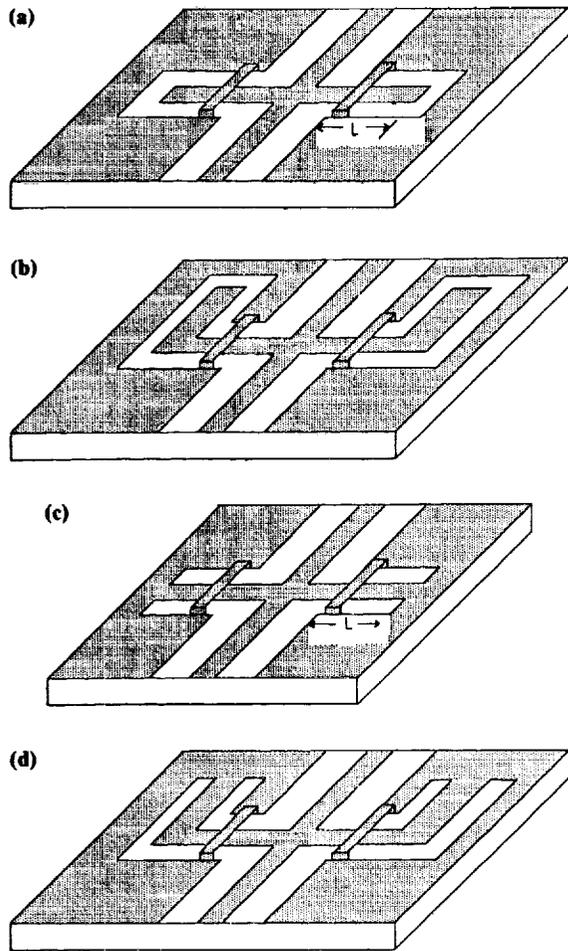
Figure 9. Different CPW shunt stubs. (a) Straight open-end CPW stub. (b) Bent open-end CPW stub. (c) Straight short-end CPW stub. (d) Bent short-end CPW stub.

Figure 10. The measured loss factor $(1 - |S_{11}|^2 - |S_{12}|^2)$ of the open-end shunt stubs (a) without air-bridges and (b) with air-bridges. $S = 75 \ \mu m$, $W = 50 \ \mu m$, $h = 400 \ \mu m$, $\epsilon_r = 13$, mean stub length $= 1100 \ \mu m$; the slots and center conductor of the stubs have equal widths of 25 μm.
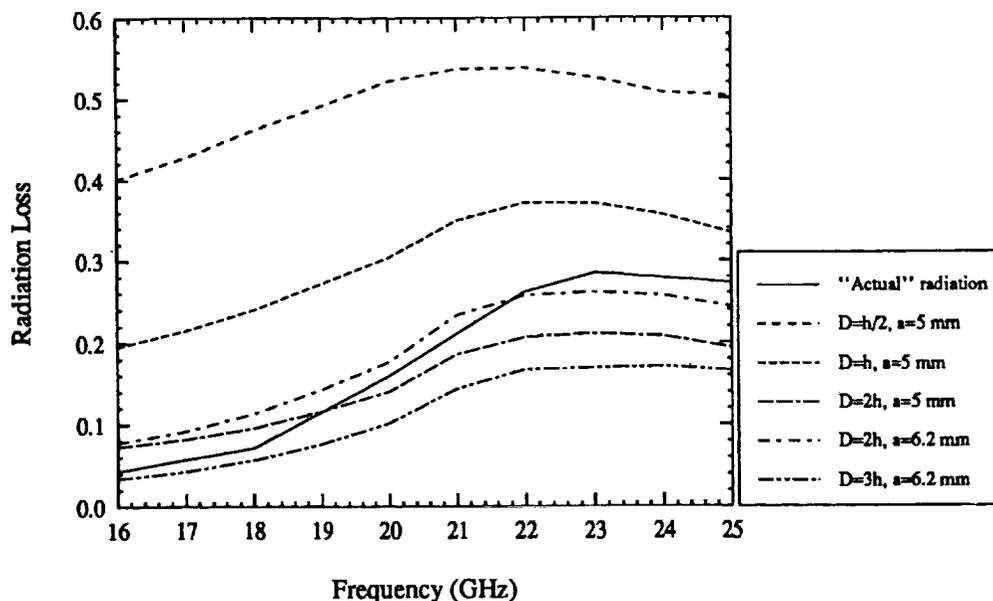
Figure 11 compares the radiation loss of a straight series stub, as predicted by setting the resistance of the top and bottom walls of the rectangular box to 377 Ω, to the "actual" radiation loss. The top and bottom walls are at a distance D from the slot aperture and the lower interface of the dielectric substrate, respectively. In addition, the parameter "a" indicates the cavity width. It can be noticed that the parameter D undoubtedly affects the final result. Furthermore, there is no specific D at which one can be sure that the predicted radiation loss is the closest to the actual one. Thus, such a simulation cannot provide any consistent results with respect to the radiation loss in printed circuits or radiation resistance in printed antennas. Nonetheless, such a simulation can still predict the resonant frequency of the circuit or antenna element.

4. CONCLUSIONS

A comparative study between open and shielded CPW discontinuities has been presented. In this study, the space domain integral equation method was used to characterize several discontinuities such as the open-end CPW and CPW series stubs. It has been found that bent CPW stubs tend to radiate less than straight ones, which makes them more appropriate for use in microwave circuits. The notion of "forced radiation" simulation has been presented in which an open structure is simulated by setting the resistances of the top and bottom walls of the shielding box to 377 Ω. The results of such a simulation have been compared

Figure 11. Forced radiation loss from a straight series stub as compared to "actual" loss. Dimensions are the same as in Figure 7.

to the "actual" radiation loss obtained rigorously. It has been found that these results are not reliable since they are considerably affected by the size of the cavity.

ACKNOWLEDGMENTS

REFERENCES

1. R. W. Jackson, "Considerations in the use of coplanar waveguide for millimeter wave integrated circuits," *IEEE Trans. Microwave Theory Tech.,* Vol. 34, Dec. 1986, pp. 1450–1456.

2. R. N. Simons and G. E. Ponchak, "Modeling of some coplanar waveguide discontinuities," *IEEE Trans. Microwave Theory Tech.,* Vol. 36, Dec. 1988, pp. 1796–1803.

3. G. Kibuuka, R. Bertenburg, M. Naghed, and I. Wolff, "Coplanar lumped elements and their application in filters on ceramic and gallium arsenide substrates," *Proc. 19th Eur. Microwave Conf.,* London, Sept. 1989, pp. 656–661.

4. C. W. Kuo and T. Itoh, "Characterization of the coplanar waveguide step discontinuity using the transverse resonance method," *Proc. 19th Eur. Microwave Conf.,* London, Sept. 1989, pp. 662–665.

5. N. Koster, S. Koblowski, R. Bertenburg, S. Heinen, and I. Wolff, "Investigation of air bridges used for MMICs in CPW technique," *Proc. 19th Eur. Microwave Conf.,* London, Sept. 1989, pp. 666–671.

6. R. W. Jackson, "Mode conversion at discontinuities in finite-width conductor-backed coplanar waveguide," *IEEE Trans. Microwave Theory Tech.,* Vol. 37, Oct. 1989, pp. 1582–1589.

7. M. Drissi, V. Fouad Hanna, and J. Citerne, "Analysis of coplanar waveguide radiating end effects using the integral equation technique," *IEEE Trans. Microwave Theory Tech.,* Vol. 39, Jan. 1991, pp. 112–116.

8. N. Dib and P. Katehi, "Modeling of shielded CPW discontinuities using the space domain integral equation method (SDIE)," *J. Electromag. Waves Appl.,* April 1991, pp. 503–523.

9. N. Dib, P. Katehi, G. Ponchak, and R. Simons, "Theoretical and experimental characterization of coplanar waveguide discontinuities for filter applications," *IEEE Trans. Microwave Theory Tech.,* May 1991, pp. 873–882.

10. M. Rittweger, M. Abdo, and I. Wolff, "Full-wave analysis of coplanar discontinuities considering three-dimensional bond wires," *1991 IEEE MTT-S Int. Microwave Symp. Dig.,* pp. 465–468.

11. N. Dib, P. Katehi, and G. Ponchak, "Analysis of shielded CPW discontinuities with air bridges," *1991 IEEE MTT-S Int. Microwave Symp. Dig.,* pp. 469–472.

12. W. Harokopus and P. Katehi, "Radiation loss from open CPW discontinuities," *1991 IEEE MTT-S Int. Microwave Symp. Dig.,* pp. 743–746.

13. M. Naghed, M. Rittweger, and I. Wolff, "A new method for the calculation of the equivalent inductances of coplanar waveguide discontinuities," *1991 IEEE MTT-S Int. Microwave Symp. Dig.*, pp. 747–750.

14. R. Bromme and R. Jansen, "Systematic investigation of CPW MIC/MMIC structures using strip/slot 3D electromagnetic simulator," *1991 IEEE MTT-S Int. Microwave Symp. Dig.*, pp. 1081–1084.

15. N. Dib and P. Katehi, "The effect of mitering on CPW discontinuities," *Proc. 21st Eur. Microwave Conf.*, Sept. 1991, pp. 223–228.

16. T. Becks and I. Wolff, "Calculation of three-dimensional passive structures including bond-wires, via-holes and air-bridges using the spectral domain analysis method," *Proc. 21st Eur. Microwave Conf.*, Sept. 1991, pp. 571–576.

17. M. Rittweger, N. Koster, S. Koblowski, R. Bertenburg, S. Heinen, and I. Wolff, "Full-wave analysis of a modified coplanar air bridge T-junction," *Proc. 21st Eur. Microwave Conf.*, Sept. 1991, pp. 993–998.

18. U. Mueller, M. Rittweger, and A. Beyer, "Coplanar short considered by the TLM-method with symmetrical condensed nodes," *Proc. 21st Eur. Microwave Conf.*, Sept. 1991, pp. 999–1003.

19. J. McClean, A. Wieck, K. Ploog, and T. Itoh, "Fullwave analysis of open-end discontinuities in coplanar stripline and finite ground plane coplanar waveguide in open environments using a deterministic spectral domain approach," *Proc. 21st Eur. Microwave Conf.*, Sept. 1991, pp. 1004–1007.

20. K. Beilenhoff, W. Heinrich, and H. Hartnagel, "The scattering behavior of air bridges in coplanar MMICs," *Proc. 21st Eur. Microwave Conf.*, Sept. 1991, pp. 1131–1135.

21. M. Naghed and I. Wolff, "Equivalent capacitances of coplanar waveguide discontinuities and interdigitated capacitors using a three dimensional finite difference method," *IEEE Trans. Microwave Theory Tech.*, Vol. 38, Dec. 1991, pp. 1808–1815.

22. C. P. Wen, "Coplanar waveguide: A surface strip transmission line suitable for nonreciprocal gyromagnetic device applications," *IEEE Trans. Microwave Theory Tech.*, Vol. 17, Dec. 1969, pp. 1087–1090.

23. M. Houdart, "Coplanar lines: Application to broadband microwave integrated circuits," *Proc. 6th Eur. Microwave Conf.*, Rome, 1976, pp. 49–53.

24. P. A. Holder, "X-band microwave integrated circuits using slotlines and coplanar waveguide," *Radio Electronics Engineering*, Vol. 48, Jan./Feb. 1978, pp. 38–42.

25. R. N. Simons, "Propagation characteristics of some novel coplanar waveguide transmission lines on GaAs at mm-wave frequencies," *1986 Conf. on Millimeter Wave/Microwave Measurements and Standards for Miniaturized Systems*, pp. 79–92.

26. G. Ghione and C. U. Naldi, "Coplanar waveguides for MMIC applications: effect of upper shielding, conductor backing, finite-extent ground planes, and line-to-line coupling," *IEEE Trans. Microwave Theory Tech.*, Vol. 35, March 1987, pp. 260–267.

27. T. Hirota, Y. Tarusawa, and H. Ogawa, "Uniplanar MMIC hybrids—a proposal of a new MMIC structure," *IEEE Trans. Microwave Theory Tech.*, Vol. 35, June 1987, pp. 576–581.

28. L. P. B. Katehi, "Novel transmission lines for the submillimeter-wave region," *IEEE Proc.* (to appear).

29. W. P. Harokopus, B. Cormanyos, L. P. B. Katehi, and G. M. Rebeiz, "Theoretical and experimental study of lens-supported aperture antennas," *IEEE Trans. Ant. Propagat.* (to appear).

30. W. P. Harokopus and P. B. Katehi, "Characterization of microstrip discontinuities on multilayer dielectric substrates including radiation losses," *IEEE Trans. Microwave Theory Tech.*, Dec. 1989, pp. 2058–2065.

31. *Sonnet Software User's Manual*, Release 2.2, Nov. 1991.

32. U. Rohde, "Improved noise modeling of GaAs FETs, Part 1: Using an enhanced equivalent circuit technique," *Microwave J.*, Nov. 1991, pp. 87–101.

33. R. F. Harrington, *Field Computation by Moment Methods*, Macmillan, New York, 1968.

34. L. P. Dunleavy and P. B. Katehi, "Generalized method for analyzing shielded thin microstrip discontinuities," *IEEE Trans. Microwave Theory Tech.*, Vol. 36, Dec. 1988, pp. 1758–1766.

35. T. E. van Deventer, P. B. Katehi, and A. C. Canggellaris, "An integral equation method for the evaluation of conductor and dielectric losses in high frequency interconnects," *IEEE Trans. Microwave Theory Tech.*, Dec. 1989, pp. 1964–1971.

36. P. B. Katehi, "A space domain integral equation approach in the analysis of dielectric-covered slots," *Radio Sci.*, Vol. 24, March/April 1989, pp. 253–260.

37. P. B. Katehi and N. G. Alexopoulos, "Real axis integration of Sommerfeld integrals with applications to printed circuit antennas," *J. Math. Phys.*, Vol. 24(3), March 1983, pp. 527–533.

38. N. Dib, G. Ponchak and L. P. Katehi, "A comprehensive theoretical and experimental study of coplanar waveguide shunt stubs," *1992 IEEE MTT-S Int. Microwave Symp.*, New Mexico, June 1992, pp. 947–950.

BIOGRAPHY

Nihad Dib received the BSc and MSc degrees in Electrical Engineering from Kuwait University in 1985 and 1987, respectively. He worked as a Laboratory Engineer in the ECE Department at Kuwait University for two years. He has been with the Radiation Laboratory, University of Michigan, since September of 1988, where he is currently working toward his PhD degree. He is a recipient of a predoctoral Rackham Fellowship, University of Michigan, during the 1991–92 academic year. His research deals mainly with the construction of CAD programs for the analysis of coplanar waveguide structures.

William P. Harokopus, Jr. was born in Detroit, Michigan, in 1963. He received his BSEE, MSEE, and PhD degrees from the University of Michigan in 1985, 1986, and 1991, respectively. From 1987–1991 he worked as a research assistant in the Radiation Lab at the University of Michigan. Duties consisted of the development of numerical techniques to study the behavior of microstrip and coplanar waveguide discontinuities and circuits. In 1991 he joined the Advanced Technology and Components Division of Texas Instruments in Mckinney, Texas. He is currently working as an antenna engineer in the Antenna/Non-Metallics Department.

George Ponchak received his BEE from Cleveland State University, Cleveland, Ohio, in 1983 and the MSEE from Case Western Reserve University, Cleveland, in 1987. He joined the NASA Lewis Research Center, Cleveland, in July of 1983 as a member of the Space Communications Division. Since joining NASA he has been engaged in research in solid-state technology development, transmission lines, and monolithic microwave integrated circuits (MMICs). He is currently pursuing his PhD degree at the University of Michigan.

Linda P. B. Katehi received the BSEE degree from the National Technical University of Athens, Greece, in 1977 and the MSEE and PhD degrees from the University of California, Los Angeles, in 1981 and 1984, respectively. In September 1984, she joined the faculty of the EECS Department of the University of Michigan, Ann Arbor. Since then, she has been involved in the modeling and computer-aided design of millimeter and near-millimeter wave monolithic circuits and antennas. In 1984 she received the W. P. King Award and, in 1985, the S. A. Schelkunoff Award from the Antennas and Propagation Society. In 1987, she received an NSF Presidential Young Investigator Award and an URSI Young Scientist Fellowship. She is a senior member of IEEE AP-S, MTT-S, and a member of Sigma Xi and URSI Commission D.